Refinability of splines derived from regular tessellations

Jörg Peters

February 27, 2014

Abstract

Splines can be constructed by convolving the indicator function of a cell whose shifts tessellate $\mathbb{R}^n$. This paper presents simple, geometric criteria that imply that, for regular shift-invariant tessellations, only a small subset of such spline families yield nested spaces: primarily the well-known tensor-product and box splines. Among the many non-refinable constructions are hex-splines and their generalization to the Voronoi cells of non-Cartesian root lattices.

1 Introduction

Univariate uniform B-splines can be defined by repeated convolution, starting with the indicator functions[1] of the intervals or cells delineated by knots. This construction implies local support and delivers a number of desirable properties (see [dB78, dB87]) that have made B-splines the representation of choice in modeling and analysis. In particular, B-splines are refinable. That is, they can be exactly represented as linear combinations of B-splines with a refined knot sequence. Refinability is a key ingredient of multi-resolution and adaptive and sparse representation of data. Refinability also guarantees monotone decay of error when shrinking the intervals.

By tensoring univariate B-splines, we can obtain splines on Cartesian grids in any dimension. Box-splines [dHR93] generalize tensoring by allowing convolution in directions other than orthogonal ones. As a prominent example in two variables, the linear 3-direction box-spline consists of linear pieces over each of six equilateral triangles surrounding one vertex [Fre71]. Shifts of this 'hat function' on an equilateral triangulation sum to one. Convolution of the hat function with itself results in a twice continuously differentiable function of degree 4; and m-fold convolution yields a function of degree $3m-2$ with smoothness C^{2m}. Since this progression skips odd orders of smoothness, van der Ville et al. [vBU$^+$04] proposed to directly convolve the indicator function of the hexagon and build splines customized

[1] An indicator function takes on the value one on the interval but is zero otherwise.

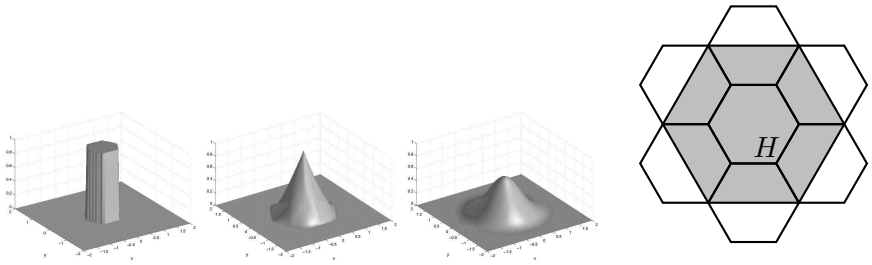

(a) hex-splines of degree 0,1,2 (b) half-scaled hex-tiling

Figure 1: (a) Splines by **convolution of the hexagonal Voronoi cell** (http://bigwww.epfl.ch/demo/hexsplines) (b) Non-nesting of the hex partition in Example 1.

to the hexagonal tessellation of the plane (cf. Fig. 1a). They went on to show that the resulting hex-splines share a number of desirable properties familiar from box-splines. But the authors did not settle whether the splines were *refinable* [vdVU10], i.e. whether hex-splines of the given hexagonal tessellation T can be represented as linear combinations of hex-splines based on a scaled-down hexagonal tessellation, say $\frac{1}{2}T$, for some choice of origin. Generalizing the analysis of hex-splines,

- this paper presents simple geometric criteria necessary for regular shift-invariant tessellations to admit refinable indicator functions.

For example, such a tessellation must contain, for every cell facet f, the whole plane, of the same dimension as f, of which f is a piece. Therefore, refinability, even of just the constant spline, strongly restricts allowable tessellations by a geometric criterion rather than algebraic or harmonic analysis.

- In contrast to tensor-product and box splines, we show that hex-splines and similar multi-variate lattice-based constructions can only be *scaled, but not refined* since scaled spaces are not nested.

The following example motivates why nested spaces and refinability are important. While nested spaces guarantee monotonically decreasing error, for non-nested spaces *halving the scale can increase the error*, even repeatedly for several scaling steps.

Example 1 Let $\mathcal{H}^i$ be the space of indicator functions over a regular tessellation by hexagons of diameter 2^{-i} and such that, at each level of scaling, the origin is the center of one hexagon. Denote by H the indicator function in $\mathcal{H}^0$ whose support hexagon is centered at the origin. $\mathcal{H}^1$ does not contain a linear combination of functions that can replicate H since the supports

of the six relevant scaled indicator functions are bisected by the boundary of the support of H (see Fig. 1b). Correspondingly, the L^2 approximation error to H from $\mathcal{H}^1$ is $\frac{6}{2}A^1 > 0$ where A^1 is the area of the hexagon with diameter $\frac{1}{2}$. Since the error from $\mathcal{H}^0$ is by construction zero, the scaling by $1/2$ has increased the error. □

By carefully adding to H an increasing number of scaled-down copies, increases in the L^2 error can be distributed over multiple scaling steps.

Overview. Section 2 reviews tessellations induced by lattices, hex-splines and their generalizations. Section 3 exhibits two non-algebraic, non-harmonic criteria – chosen for their simplicity – for testing whether a tessellation can support a refinable space of splines that are constructed by convolution of indicator functions of its cells.

2 Splines from lattice Voronoi cells

An n-dimensional lattice is a discrete subgroup of full rank in an n-dimensional Euclidean vector space. Alternatively, such a lattice may be viewed as inducing a tessellation of space into identical cells without n-dimensional overlap[2]. The tessellation is then generated by the translational shifts of one cell. In particular, lattice points can serve as sites of Voronoi cells (nearest-neighbor regions). The Euclidean, $n = 2$ plane admits three highly symmetric tessellations. The regular tessellation into squares can be associated with uniform tensor-product B-splines [dB78], the hexagonal partition with the bivariate hat function of the Introduction and, if we allow for two types of regular triangles, say 'up' $\triangle$ and 'down' $\triangledown$, the regular triangulation can be associated with half-box splines [PB02].

An interesting additional type of spline arises from convolving the indicator function H of the hexagon with itself. Such hex-splines, a family of C^{k-1} splines supported on a local $k+1$-neighborhood, were developed and analyzed by van De Ville et al. [vBU$^+$04] (see Fig. 1a). That paper compares hex-splines to tensor-product splines and uses the Fourier transform of hex-splines to derive, for low frequencies, the L^2 approximation order, as a combination of the projection into the hex-spline space and a quasi-interpolation error. [CvB05] derived quasi-interpolation formulas and showed promising results when applying hex-splines to the reconstruction of images (see also [CvU06, Cv07, Cv08]). Van De Ville et al. [vBU$^+$04] also observed that hexagons are Voronoi cells of a lattice and that the cell can be split into three quadrilaterals, using one of two choices of the central split. Thus H can be split into three constant box splines whose mixed convolution yields higher-order splines. This approach has been generalized to Voronoi

[2] A common convention is to define the cells to be half-open sets so that they do not overlap on facets, but nevertheless cover.

cells of the face-centered cubic (FCC, see Fig. 2a)) and body-centered cubic (BCC) lattices [Kim08b, ME10], and can be extended to more general lattices. Of particular interest are the non-Cartesian crystallographic root lattices $\mathcal{A}_n$, $\mathcal{D}_n$, in n dimensions, and their duals $\mathcal{A}_n^*$, $\mathcal{D}_n^*$, as well as highly symmetric lattices $\mathcal{E}_j$, in dimensions $j = 6, 7, 8$ (cf. [CS98, Ch 4]). These lattices provide more isotropic tessellations, i.e. with sphere-like uniformity in all directions, than the Cartesian grid (Fig. 2 shows two lattices in $\mathbb{R}^3$). Starting with [PM62], crystallographic root lattices have therefore repeatedly been proposed for sampling and signal processing.

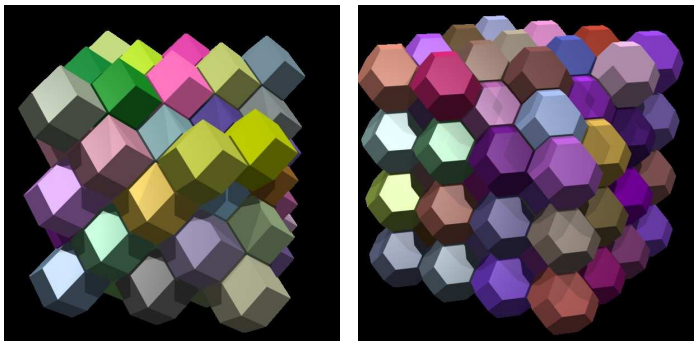

(a) Rhombic dodecahedra (b) Truncated octahedra

Figure 2: The **Voronoi tessellations** associated with $\mathcal{A}_3$ (FCC) and $\mathcal{A}_3^*$ (BCC) (from http://en.wikipedia.org/wiki/Honeycomb_geometry). See also Fig. 4.

3 Refinability constraints

We consider a polyhedral tessellation T of $\mathbb{R}^n$ into n-dimensional, unpartitioned units, called *cells*. Cells are bounded by a finite number of $n-1$-dimensional *facets*. We denote by $\chi(T)$ the space of indicator functions of the cells of T and by $\chi(T^1)$ the space of indicator functions on some uniformly scaled-down copy T^1 of T. The space $\chi(T)$ is *refinable* if each indicator function in $\chi(T)$ can be represented as a linear combination of functions in $\chi(T^1)$, for some choice of scaling center. Proposition 1 below provides a *necessary condition* that avoids the need for algebraic or harmonic analysis. While our focus is on shift-invariant tessellations, Proposition 1 applies more generally and also to cell boundaries of co-dimension greater than 1. Its proof uses the notion of a cell $c^1 \in T^1$ straddling a facet of a cell $c \in T$. A cell c^1 *straddles* a facet f of c if there exists a point $\mathbf{p}$ on f, a unit vector $\mathbf{n}$ normal to f at $\mathbf{p}$ and $\epsilon > 0$ such that both $\mathbf{p} + \epsilon\mathbf{n} \in c^1$ and $\mathbf{p} - \epsilon\mathbf{n} \in c^1$.

Proposition 1 *Let T be a polyhedral tessellation of $\mathbb{R}^n$ and T^1 its scaled-down copy. Then $\chi(T)$ is refinable only if every facet of T is the union of*

facets of T^1.

Proof Assume that a facet f of a cell c in T is not a union of facets of T^1. Then, since T^1 is a tessellation, some cell c^1 of T^1 must straddle f. Let $H^1 \in \chi(T^1)$ be the indicator function of c^1 and H the indicator function of c. Then, in order to reproduce the unit step of H across f, H^1 must simultaneously take on both the value 0 and the value 1. |||

Translation-invariant or shift-invariant tessellations are a special case of transitive tilings where every cell can be mapped to every other cell by translation, without rotation.

Proposition 2 *If T is a shift-invariant tessellation, $\chi(T)$ is refinable only if T contains, for each facet f, the hyperplane through f as a union of its facets.*

Proof The coarser-scaled copies of T contain enlarged copies of every facet in T. By Proposition 1 these copies must be a union of facets of T. Therefore a *shifted copy* of every facet is strictly contained in the interior of and so extended by some coarser facet. Shift-invariance then implies that *every* facet f lies strictly inside such an extension. Ever coarser tessellations provide a sequence of extensions of f in any direction by any amount. |||

Of the three regular tessellations of the plane, only the Cartesian grid satisfies the assumptions of Proposition 2. The regular triangulation satisfies the hyperplane constraint, but requires reflection to map $\triangle$ into $\triangledown$, i.e. is not a shift-invariant tessellation of one type of triangle. The partition into hexagons is shift-invariant, but does not contain the required hyperplanes. We conclude that

Corollary 1 *Hex splines are not refinable.*

We can generalize this observation by simplifying the inspection criterion.

We say that two abutting facets f_1 and f_2 of a cell c *meet with an obtuse angle* if, for $i = 1, 2$, there exist unit vectors $\mathbf{n}_i$ orthogonal to f_i and outward pointing so that $\mathbf{n}_1 \cdot \mathbf{n}_2 > 0$.

Proposition 3 *Let T be a tessellation of $\mathbb{R}^n$ by shifts of one polyhedral cell c. If two facets f_1 and f_2 of c meet with an obtuse angle and if the reflection c' of c across the plane through f_2 is a cell of T then $\chi(T)$ is not refinable.*

Proof Assume $\chi(T)$ is refinable under the given conditions. Denote by f_1' the reflection of f_1 across the plane through f_2 and by e the common intersection of f_1, f_2 and f_1' (see Fig. 3). Since c' must not overlap c, no facet of c can meet f_2 with an angle exceeding π (such as the reentrant corner of an L-shaped cell). By Proposition 2 the extension F_1 of f_1 lies in T. Since the outward-pointing normal of f_2 with respect to c' is $-\mathbf{n}_2$, f_2 and F_1 meet at e with an acute angle: $\mathbf{n}_1 \cdot (-\mathbf{n}_2) < 0$. However, within c',

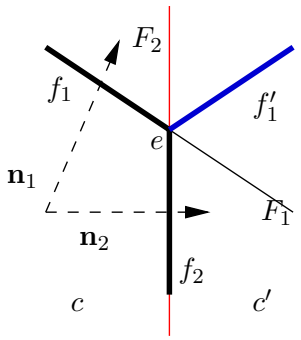

Figure 3: A pair of facets f_1, f_2 of a cell c meet at e with an **obtuse angle**: the outward pointing normals $\mathbf{n}_1$, $\mathbf{n}_2$ (dashed) have a strictly positive inner product.

by reflection, the facets f_2 and f_1' meet at e with an obtuse angle. Therefore F_1 extends f_1 into c' and splits c'. This contradicts the definition of a cell as an unpartitioned unit. |||

Proposition 3 helps decide which of the (symmetric crystallographic) root lattices $\mathcal{A}_n$, $\mathcal{A}_n^*$, $\mathcal{B}_n$, $\mathcal{D}_n$, $\mathcal{D}_n^*$, $\mathcal{E}_j$, $j = 6, 7, 8$ [CS98] are suitable for building refinable splines by convolution of their Voronoi cells. [CS98, 21,3] characterizes the Voronoi cells of crystallographic root lattices in terms of fundamental cones, the fundamental simplex, extended Coxeter-Dynkin diagrams and Wythoff's construction. However, the following proof is based on more elementary notions.

Corollary 2 (root lattices) *Splines obtained by convolving the Voronoi cell of a non-Cartesian crystallographic root lattice are not refinable.*

Proof By definition, crystallographic lattices satisfy the reflection assumption of Proposition 3. We need only determine whether the Voronoi cells of the root lattices contain a pair of facets that meet with an obtuse angle, the obtuse-angle assumption of Proposition 3. Choosing one Voronoi site (cell center) as the origin, we will exhibit, for each lattice, two lattice points, $\mathbf{n}_1$ and $\mathbf{n}_2$, that contribute Voronoi facets f_1 and f_2 (that are pieces of bisector hyper-planes h_1 and h_2) to the central Voronoi cell and such that $\mathbf{n}_1 \cdot \mathbf{n}_2 > 0$. It is possible that f_1 and f_2 do not meet, because other lattice points contribute Voronoi facets that separate the intersection of h_1 and h_2 from the Voronoi cell. If so, let $\mathbf{p} := \alpha\mathbf{n}_1 + \beta\mathbf{n}_2$ be the intersection point of h_1, h_2 in the plane spanned by $\mathbf{n}_1$ and $\mathbf{n}_2$. Since $\mathbf{n}_1 \cdot \mathbf{n}_2 > 0$, $0 < \alpha, \beta < 1/2$. Let $\mathbf{n}_k$ be a lattice point whose Voronoi facet f_k separates $\mathbf{p}$ from the Voronoi cell of the origin. Let $\mathbf{n}_k x = 2r_k$ be the plane equation of f_k. Since $\mathbf{n}_1$ and $\mathbf{n}_2$ contribute Voronoi cells $\mathbf{n}_k \cdot \mathbf{n}_j/2 < 2r_k$. Since $\mathbf{p}$ is outside, $\mathbf{n}_k \cdot \mathbf{p} > 2r_k$ must hold. But this can only hold if $\mathbf{n}_j \cdot \mathbf{n}_k > 0$ for $j = 1, 2$. Since the number of facets is finite, checking the neighbors with

the maximal inner product and inserting any additional Voronoi facets must yield a pair of facets that *meet* with an obtuse angle.

The $\mathcal{A}_n$ lattice is traditionally defined via an embedding in $\mathbb{R}^{n+1}$, $n > 1$. More convenient for our purpose is the alternative geometric construction in $\mathbb{R}^n$ via the $n \times n$ generator matrix $\mathbf{A}_n := \mathbf{I}_n + \frac{c_n}{n}\mathbf{J}_n$ of Theorem 1 of [KP10]. Here $\mathbf{I}_n$ is the identity matrix, $\mathbf{J}_n$ the $n \times n$ matrix of ones and $c_n := \frac{-1+\sqrt{n+1}}{n}$. Let $\mathbf{j}$ be the vector all of whose entries are 1 and $\cdot$ denote the scalar product of vectors. Since $\frac{1}{2} > \frac{c_n}{n}(2 + c_n) > 0$ for $n > 1$, among elements $\mathbf{x} \in \mathbb{Z}^n \backslash \mathbf{0}$, $\|\mathbf{A}_n\mathbf{x}\|^2 = \|\mathbf{x}\|^2 + \frac{c_n}{n}(2 + c_n)(\mathbf{j} \cdot \mathbf{x})^2$ is minimized by choosing $\mathbf{x}$ to be any ith coordinate vector $\mathbf{e}_i$. Therefore $\mathbf{A}_n\mathbf{e}_i$ is a nearest lattice point to the origin and Voronoi site, i.e. it contributes a facet to the Voronoi cell (cf. Fig. 4c,d) and for $i \neq j$

$$\mathbf{A}_n\mathbf{e}_i \cdot \mathbf{A}_n\mathbf{e}_j = \frac{c_n}{n}(2 + c_n) > 0.$$

For the $\mathcal{A}_n^*$ lattice, the generator matrix is $\mathbf{A}_n^* := \mathbf{I}_n + \frac{c_n^*}{n}\mathbf{J}_n$ with $c_n^* := -1 \pm \frac{1}{\sqrt{n+1}}$ so that $\|\mathbf{A}_n^*\mathbf{x}\|^2 = \|\mathbf{x}\|^2 - \frac{1}{n+1}\mathbf{x}^T\mathbf{J}_n\mathbf{x}$. While $\mathbf{e}_i$ minimizes $\|\mathbf{A}_n^*\mathbf{x}\|^2$ over the integer vectors, by duality, the inner product of $\mathbf{A}_n^*\mathbf{e}_i$ and $\mathbf{A}_n^*\mathbf{e}_j$ is not positive for $i \neq j$. However, since $\|\mathbf{A}_n^*\mathbf{e}_i\|^2 = \frac{n}{n+1} = \|\mathbf{A}_n^*\mathbf{j}\|^2$, $\mathbf{A}_n^*\mathbf{j}$ is also a nearest lattice neighbor. The claim then follows from

$$\mathbf{A}_n^*\mathbf{e}_1 \cdot \mathbf{A}_n^*\mathbf{j} = (\mathbf{e}_i + \frac{c_n^*}{n}\mathbf{j}) \cdot (\mathbf{j} + c_n^*\mathbf{j}) = 1 + 2c_n^* + (c_n^*)^2 = \frac{1}{n+1} > 0.$$

For the $\mathcal{D}_n$ lattice, defined in $n \geq 3$ dimensions, a generator matrix is $\mathbf{D}_n := \begin{bmatrix} \mathbf{I}_{n-1} & -\mathbf{e}_{n-1}^{n-1} \\ -\mathbf{j}_{n-1}^t & -1 \end{bmatrix}$ (see e.g. Section 7 of [KP11]). Among lattice points, the points $\mathbf{D}_n\mathbf{e}_i$, $i \leq n$, yield the minimal squared norm of 2. For $i < j < n$,

$$\mathbf{D}_n\mathbf{e}_i \cdot \mathbf{D}_n(\mathbf{e}_j) = (\mathbf{e}_i + \mathbf{e}_n) \cdot (\mathbf{e}_j + \mathbf{e}_n) = 1 > 0.$$

A generator matrix of $\mathcal{D}_n^*$ is $\mathbf{D}_n^* := \begin{bmatrix} \mathbf{I}_{n-1} & \mathbf{j}_{n-1}/2 \\ \mathbf{0}^t & 1/2 \end{bmatrix}$ indicating that $\mathcal{D}_n^*$ is the union of $\mathbb{Z}^n$ and hypercube centers $\mathbf{j}/2 + \mathbb{Z}^n$. For $n = 3$, the root vectors whose entries are $\pm 1/2$ are nearest and $(1, 1, 1) \cdot (1, 1, -1) > 0$ confirms the claim. For $n = 4$, hypercube centers and axis neighbors have the least norm and $(1, 1, 1, 1)/2 \cdot (1, 0, 0, 0) > 0$ confirms the claim. For $n > 4$, only the vectors $\mathbf{e}_i$, $i < n$ have the least norm. But the intersections of the half-spaces, bisecting the (root) vectors $\mathbf{e}_i$ from the origin, forms a hypercube and the hyper-cube corner $\mathbf{j}$ is never closer to the origin than $\mathbf{j}/2$. Therefore the Voronoi diagram is determined not just by the nearest neighbors $\mathbf{e}_i$, but also by second nearest neighbors, namely $\mathbf{j}/2$ for $4 < n \leq 8$ and $\mathbf{e}_i + \mathbf{e}_j$, $i < j < n$ for $n > 8$. Observing that $\mathbf{e}_1 \cdot \mathbf{j}/2 > 0$ and $(\mathbf{e}_1 + \mathbf{e}_2) \cdot \mathbf{e}_1 > 0$ proves the claim.

For $\mathcal{B}_n$, the Cartesian cube lattice has an inner product of 0. Indeed, its uniform tensor-product B-spline constructions are refinable. On the other

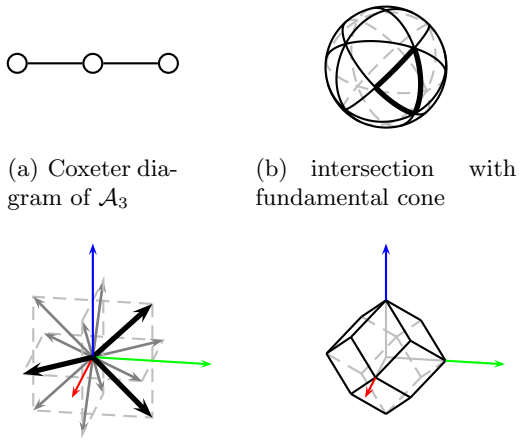

(a) Coxeter diagram of $\mathcal{A}_3$

(b) intersection with fundamental cone

(c) 12 root vectors of $\mathcal{A}_3$

(d) Voronoi cell: rhombic dodecahedron

Figure 4: The $\mathcal{A}_3$ **root system and Voronoi cell** of the FCC lattice (from [Kim08a]). Thick arcs in (b) indicate the intersection of the sphere and the fundamental cone spanned by the mirror planes orthogonal to the three thick-set root vectors in (c). As indicated by the Coxeter diagram (a), the dihedral angles of the cone are $\{\pi/2, \pi/3, \pi/3\}$: $\pi/3$ yields a single line, $\pi/2$ none. The 12 root vectors $\{\mathbf{e}_i \pm \mathbf{e}_j : 1 \leq i \neq j \leq 3\}$ in (c) point to nearest FCC lattice points and are orthogonal to the 12 faces of the Voronoi cell in (d).

hand, splitting each cube by adding the diagonal directions of the full root system [PW97, Kim08a] yields nearest neighbors $\mathbf{e}_i$. As for $\mathcal{D}_n^*$, the Voronoi cell is determined also by second nearest neighbors, namely $\mathbf{j}$ for $2 < n \leq 4$ (with the inner product $\mathbf{e}_1 \cdot \mathbf{j} = 1$) and $\mathbf{e}_i + \mathbf{e}_j$ for $i < j$, $n > 4$ (with the inner product $(\mathbf{e}_1 + \mathbf{e}_2) \cdot \mathbf{e}_1 = 1$).

For $\mathcal{E}_6$, we select the nearest neighbor root vectors $(1, 1, 0, 0, 0, 0)$ and $(1, 1, 1, 1, 1, \sqrt{3})/2$ of squared norm 2 and with inner product 1. For $\mathcal{E}_7$, we select the nearest neighbor root vectors $(1, 1, 0, 0, 0, 0, 0)$ and $(1, 1, 1, 1, 1, 1, \sqrt{2})/2$ of squared norm 2 and with inner product 1. For $\mathcal{E}_8$, we select the nearest neighbor root vectors $(1, 1, 0, 0, 0, 0, 0, 0)$ and $\mathbf{j}_8/2$ of squared norm 2 and with inner product 1. |||

The equilateral triangulation in $\mathbb{R}^2$ (dual to the 'honeycomb lattice' and not a standard lattice due to the flip from $\triangle$ to $\triangledown$) has an inner product of $\frac{-1}{2}$ compatible with refinability.

Remark. The interpretation of the extended Coxeter-Dynkin diagrams presented in [CS98, 21,3] and illustrated in Fig. 4 for $\mathcal{A}_3$, yields, for the crystallographic root lattices, $\mathcal{A}_n$, $\mathcal{D}_n$, $\mathcal{E}_j$, $j = 6, 7, 8$, the following succinct alternative proof of obtuse angles in Corollary 2. Since the extension node

$\tilde{\mathbf{n}}$ of each Coxeter-Dynkin diagram of each of $\mathcal{A}_n$, $\mathcal{D}_n$, $\mathcal{E}_j$ is connected to some other node $\mathbf{n}_j$ of the diagram by a single line, reflection across the plane through the facet of the fundamental simplex corresponding to $\mathbf{n}_j$ maps the Voronoi (simplex roof) facet of $\tilde{\mathbf{n}}$ to an adjacent Voronoi facet that joins it with twice the angle $\pi/3$, and hence an obtuse angle.

4 Generalizations and Conclusion

The technical report [Pet12, Sec 4] explores whether a superposition of several families of hex-splines is refinable. Specifically, if $\{T_j\}_{j=0..J}$ is a family of distinct shift-invariant tessellations obtained by shifts of some T_0, the technical report investigates whether each member of the family can be expressed as a linear combination of the scaled-down copies of splines of the family. Since the outcome for families on non-Cartesian root lattices is also negative, and since the proofs are technical and intricate, this material is not included here.

Proposition 2 fails for transitive tilings that allow for rotation. For example, let T be the L-triomino tiling. Since four L-triominos pack into one double-sized L-triomino, $\chi(T)$ is refinable. However, the full hyperplanes through the facets f_1 and f_2 forming the reentrant angle of the L-triomino are not contained in T since f_1 and f_2 are never *strictly* contained in a coarse L-triomino: they always include the end-point of any coarser facet edge. Similarly, trapezoid tessellations show that Proposition 2 fails for transitive tilings that allow for reflection. A good question is whether a proposition similar to Proposition 2 can be formulated to address refinement of more general transitive tilings.

The paper identified several necessary criteria for tessellations to admit a refinable space of (convolutions of) indicator functions. The criteria were chosen for their simplicity. For example, we showed that admissible shift-invariant tessellations must contain, for every facet, the whole plane of which the facet is a piece of the same dimension. Already for hex-splines an alternative algebraic proof of non-refinability is considerably more complicated.

Other than their innate beauty, increased isotropy of their Voronoi cells is a major reason for considering non-Cartesian root lattices: these lattices have high packing densities that can improve sampling efficiency [PM62]. Unfortunately, Corollary 2 shows that exactly this increased isotropy prevents refinability of splines via cell convolution.

In conclusion, if we seek shift-invariant refinable classes of splines from convolving indicator functions of polyhedral cells, remarkably few options exist apart from tensor-product B-splines and box-splines. In particular, the approach of convolving non-Cartesian lattice Voronoi cells fails to provide the important spline property of refinability. This does not imply that more

general lattices fail to have associated refinable splines representing their symmetry and translational structure. In the bivariate setting, odd orders of continuity on the hexagonal dual of the regular triangulation can be filled in by half-box splines [PB02]. Moreover, if fractal support is acceptable, [OS03, HR02] provide refinable functions with approximately hexagonal footprint. Combining families of symmetric box-splines, such as [KP11], yields refinable splines for any level of smoothness and crystallographic structure.

Acknowledgement Andrew Vince, Carl de Boor and Minho Kim helped me clarify parts of the exposition. The work was supported by NSF Grant CCF-1117695.

References

[CS98] J. H. Conway and N. J. A. Sloane. *Sphere Packings, Lattices and Groups*. Springer-Verlag New York, Inc., New York, NY, USA, 3rd edition, 1998.

[Cv07] L. Condat and D. van de Ville. Quasi-interpolating spline models for hexagonally-sampled data. *IEEE Trans. Image Processing*, 16(5):1195–1206, May 2007.

[Cv08] L. Condat and D. van de Ville. New optimized spline functions for interpolation on the hexagonal lattice. In *ICIP*, pages 1256–1259, 2008.

[CvB05] L. Condat, D. van de Ville, and T. Blu. Hexagonal versus orthogonal lattices: A new comparison using approximation theory. In *ICIP*, pages III: 1116–1119, 2005.

[CvU06] L. Condat, D. van de Ville, and M. Unser. Efficient reconstruction of hexagonally sampled data using three-directional box-splines. In *ICIP*, pages 697–700, 2006.

[dB78] C. de Boor. *A Practical Guide to Splines*. Springer, 1978.

[dB87] C. de Boor. B-form basics. In G. Farin, editor, *Geometric Modeling: Algorithms and New Trends*, pages 131–148. SIAM, 1987.

[dHR93] C. de Boor, K. Höllig, and S. Riemenschneider. *Box splines*. Springer-Verlag New York, Inc., New York, NY, USA, 1993.

[Fre71] L. Frederickson. Triangular spline interpolation / generalized triangular splines. Technical Report no. 6/70 and 7/71, Dept. of Math., Lakehead University, Canada, 1971.

[HR02] B. Han and S. Riemenschneider. Interpolatory biorthogonal wavelets and cbc algorithm. In *Wavelet Analaysis and Its Applications, D. Deng, D. Huang, R.Q. Jia, W. Lin, J Wang, Eds*, pages 119–139. AMS, 2002.

[Kim08a] M. Kim. *Symmetric box-splines on root lattices*. PhD thesis, University of Florida, August 2008.

[Kim08b] M. Kim. E-mail and pdf draft to A Entezari and J Peters, April 09 2008.

[KP10] M. Kim and J. Peters. Symmetric box-splines on the $\mathcal{A}_n^*$ lattice. *J. of Approximation Theory*, 162(9):1607–1630, September 2010.

[KP11] M. Kim and J. Peters. Symmetric box-splines on root lattices. *Journal of Computational and Applied Mathematics*, 235(14):3972–3989, May 2011.

[ME10] M. Mirzargar and A. Entezari. Voronoi splines. *IEEE Transactions on Signal Processing*, 58(9), 2010.

[OS03] P. Oswald and P. Schröder. Composite primal/dual -subdivision schemes. *Computer Aided Geometric Design*, 20(3):135–164, 2003.

[PB02] H. Prautzsch and W. Boehm. Box splines. *Handbook of Computer Aided Geometric Design*, Gerald Farin and Josef Hoschek and Myung-Soo Kim and Josef Hoschek and Myung-Soo Kim(Elsevier):255–282, 2002.

[Pet12] Jörg Peters. Refinabillity of splines derived from regular tessellations. Technical report, http://arxiv.org/abs/1210.5532, University of Florida, Dept CISE, December 2012.

[PM62] D. P. Petersen and D. Middleton. Sampling and reconstruction of wave-number-limited functions in N-dimensional Euclidean spaces. *Information and Control*, 5(4):279–323, December 1962.

[PW97] J. Peters and M. Wittman. Box-spline based CSG blends. In W. Bronsvort C. Hoffmann, editor, *Proceedings of Fourth Symposium on Solid Modeling*, pages 195–206. ACM Siggraph, May 1997.

[vBU+04] D. van de Ville, T. Blu, M. Unser, W. Philips, I. Lemahieu, and R. van de Walle. Hex-splines: a novel spline family for hexagonal lattices. *IEEE Trans. Image Proc.*, 13(6):758–772, June 2004.

[vdVU10] D. van de Ville and M. Unser. Personal communication, Banff, Nov 2010.